A Three-Dimensional Laser Scanning-Based Method for Dimensional Inspection of Large-Scale High-Speed Railway Precast Box Girders

Zhiguo Zhang , Shihao Dou * , Shaopeng Zhang , Kang Chen

Posted Date: 11 May 2026

doi: 10.20944/preprints202605.0620.v1

Keywords: high-speed railway prefabricated box girder; exterior dimensional inspection; 3D laser scanning; point cloud data

 doi:10.20944/preprints202605.0620.v1

Article

A Three-Dimensional Laser Scanning-Based Method for Dimensional Inspection of Large-Scale High-Speed Railway Precast Box Girders

Zhiguo Zhang [1], Shihao Dou [1,*], Shaopeng Zhang [2] and Kang Chen [1]

[1] School of Civil Engineering, Shijiazhuang Tiedao University, Shijiazhuang 050043, China

[2] China Railway Design Corporation, Tianjin 300142, China

* Correspondence: xl8068667@gmail.com;18830192176

Abstract

We present a 3D laser-scanning method for fast, accurate dimensional inspection of large high-speed-rail precast box girders. The pipeline uses low-pass filtering plus sequential registration to suppress noise, and voxel filtering with curvature-aware enhancement to reduce point-cloud size by 3–5× while preserving key geometry. Reconstruction employs K-nearest-neighbors and PCA to detect boundaries and curvature jumps, B-spline fitting with moving least squares for surface completion, and CSS corner detection to extract key dimensions at millimeter precision. Field tests report absolute errors ≤2.0 mm versus manual measurement, validating the method for automated, digital acceptance.

Keywords: high-speed railway prefabricated box girder; exterior dimensional inspection; 3D laser scanning; point cloud data

1. Introduction

Prefabricated simply supported box girders, due to their advantages of high stiffness, good integrity, and short construction periods [1,2], are the preferred structural form for bridge construction in China's high-speed rail network. They currently account for over 95% of the commonly used span simply supported beams in prefabricated erection [3]. As the standards for passen-ger-dedicated rail lines continue to evolve, higher demands are placed on construction quality and the accuracy of exterior dimensions. For example, excessive deviation in prefabricated girder length can affect the erection quality and lead to issues with expansion joints; insufficient concrete wall thickness reduces the protective layer depth, making reinforcement more susceptible to corrosion and spalling, which in turn compromises the durability and safety of the structure and increases operation and maintenance costs. Therefore, precise control over the overall and cross-sectional dimensions of prefabricated girders is critical.

Current dimensional inspection of prefabricated high-speed-railway girders predominantly relies on traditional contact measurement tools such as steel tape measures, calipers, and leveling instruments. These manual inspection methods exhibit three notable shortcomings [4]: first, sin-gle-point contact measurements are inefficient and cannot meet the time-efficiency requirements of industrialized, batch production; second, the intrinsic accuracy limits of mechanical gauges, compounded by operator-dependent variability, undermine data reliability; third, conventional approaches capture only local geometric parameters and are therefore incapable of producing comprehensive, full-feature digital models of the girder. In this context, three-dimensional (3D) laser scanning, owing to its non-contact, full-surface measurement capability and high-density point-cloud acquisition, offers an innovative solution for high-precision quantitative analysis of engineering geometry [5,6]. Field applications have demonstrated successful deployments of this technology in deformation monitoring of high-speed-railway tunnels and 3D modeling of large underground

 doi:10.20944/preprints202605.0620.v1

spaces, delivering millimeter-level accuracy and comprehensive feature coverage; consequently, 3D laser scanning has become a key enabler of the surveying profession's transition from two-dimensional to three-dimensional digital workflows [7,8], and provides a viable intel-ligent method for dimensional inspection of prefabricated high-speed-railway girders.

With the rapid development of three-dimensional (3D) laser scanning, research on its engineering applications has been primarily concentrated on geometric feature analysis [9,10]. The technological framework centers on reverse modeling, whereby high-precision point-cloud data are used to reconstruct structural geometry and thus enable millimeter-level resolution of engineering parameters [11,12]. In the field of dimensional inspection for prefabricated concrete box girders used in high-speed rail, studies employing laser point-cloud scanning for outer-contour recognition and appearance-dimension measurement hold considerable engineering value [13]. Existing work indicates that point-cloud-based reverse modeling and feature-extraction techniques offer innovative alternatives to conventional contact-based measurement methods for prefabricated box girders [14,15]. For example, Song et al. [16] constructed a 3D point-cloud model of a 30 m highway concrete small box girder and applied surface-fitting analysis to identify section dimensions; however, their approach strongly depends on point-cloud completeness and does not address re-construction of missing regions. Wang et al. [17] developed a hybrid-pixel segmentation algorithm that, by optimizing edge-detection thresholds, substantially improves the geometric accuracy of boundary recognition for complex components, providing useful guidance for exterior-feature identification of large concrete elements. Zhao et al. [18] proposed a density-adaptive compression algorithm that effectively suppresses feature degradation in low-density regions and achieved an absolute error of 1.34 mm in the inspection of prefabricated concrete elements sized 400 mm × 400 mm × 600 mm, although its effectiveness for large-scale concrete components remains to be val-idated. Wu et al. [19] attempted to establish a full-process detection system for box girders but were unable to obtain complete 3D reconstruction because of missing point-cloud data on the bottom and top faces. Wang et al. [20] exposed limitations of uniform-grid compression algorithms in large-component inspection, showing that area-calculation error grows nonlinearly with increasing component size. Synthesizing current findings, significant technical bottlenecks remain in com-plex-surface reconstruction, multi-station data-registration accuracy, and the reconstruction of missing regions. In practical engineering, laser scanning of large high-speed-rail prefabricated box girders frequently encounters complex conditions—such as off-nominal girder posture and occlu-sion by support structures—that exacerbate these issues. Moreover, the literature on dimensional inspection of large high-speed-rail prefabricated box girders is still sparse; most existing experi-mental studies target small components, which constrains the technology's large-scale deployment in engineering practice.

Building on existing studies and motivated by inspection requirements for large prefabricated box girders in high-speed railway yards, we developed a comprehensive end-to-end technical system that integrates point-cloud acquisition, data processing, and dimensional identification. The system was validated on a representative engineering project, enabling automated reconstruction of large prestressed concrete box-girder models and automatic extraction of principal dimensional parameters to support acceptance testing. This work provides theoretical foundations and technical support for the intelligent construction and prefabricated assembly of high-speed-railway components.

2. Full-Process Inspection System for Large-Scale High-Speed Rail-way Prefabricated Box Girders

Accurate measurement of key parameters—such as span length and cross-sectional dimensions—during the acceptance stage of prefabricated high-speed-rail box girders constitutes the primary basis for product delivery. Conventional inspections, which rely on manual, contact-based instruments, suffer from low efficiency, numerous measurement blind spots, and incomplete data coverage, rendering them inadequate for the quality requirements of intelligent construction. Furthermore, storage areas within prefabrication yards are spatially constrained; the box girders

 doi:10.20944/preprints202605.0620.v1

themselves commonly exhibit an upward camber induced by prestressing, the top faces are densely occupied by embedded reinforcement, and the end regions feature protruding prestressing tendons and anchorage devices—all of which further complicate measurement. Therefore, the development of a fully automated, end-to-end inspection system—comprising system deployment, data acquisition, point-cloud preprocessing, point-cloud feature recognition and missing-region reconstruction, and dimensional identification—represents a critical breakthrough for improving box-girder quality control and expanding applications of intelligent construction.

To address the current limitations of point-cloud detection technology—namely, the severe point cloud loss caused by occlusion from construction facilities and densely arranged double-layer beam storage in the data acquisition process; the insufficient adaptability of existing reconstruction algorithms for the beam's non-fixed deflection surface characteristics; and the reliance on manual intervention in the dimensional extraction process, leading to fragmented workflows and poor structural repeatability—this study develops a full-process inspection system as shown in Figure 1. First, a dynamic measurement station location optimization strategy for 3D laser scanning is established, which, combined with the spatial characteristics of the prefabricated beam yard and the geometric properties of the box girder, effectively avoids detection blind spots and significantly improves point cloud coverage. Second, a multimodal point cloud optimization method integrating low-pass filtering and sequential registration is developed to suppress noise from concrete surface textures while retaining key fine features, thereby improving data preprocessing efficiency and stability. Building on this, boundary points and curvature discontinuities are extracted based on K-NN and PCA algorithms. For areas prone to missing data, such as the bottom slab and flange, B-spline curves and the MLS method are introduced for joint modeling, enabling deflection surface reconstruction that accounts for prestressing effects and symmetry repair. Furthermore, a hierarchical slicing method driven by geometric constraints, combined with CSS feature extraction, is employed to achieve millimeter-level automatic detection of six critical dimensions, including beam length, deck width, and web thickness. This system significantly reduces manual involvement, increasing detection efficiency by approximately three times compared to manual methods. It effectively resolves the traditional issues of "experience-driven and inefficient" inspections, reducing the risk of beam misalignment caused by dimensional deviations.

Compared with existing studies, this work is the first to achieve a deep coupling between multi-scale geometric processing algorithms and the practical constraints of large-scale railway prefabricated box girders. It advances the inspection paradigm from passive spot-checking to active, full-feature analysis, and provides a more systematic, intelligent, and reusable technical pathway for high-precision dimensional control of prefabricated components in high-speed rail projects.

 doi:10.20944/preprints202605.0620.v1

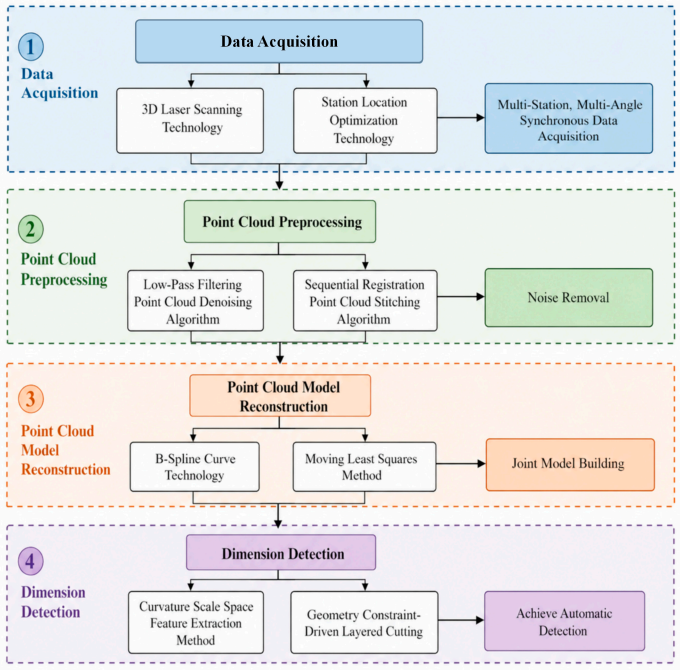

Figure 1. Overall workflow of the full-process inspection for prefabricated box girders.

3. Point Cloud Preprocessing Technology for Large-Scale High-Speed Railway Box Girders

During the three-dimensional laser scanning of large-scale high-speed railway precast box girders, point cloud acquisition is subject to multiple constraints arising from both the spatial layout of the storage yard and the geometric characteristics of the girders themselves. Owing to the complex geometry, surface reflectivity, and on-site environmental conditions, the raw point cloud data often exhibit noise, non-uniform density, and local data voids. Therefore, preprocessing of the raw point cloud is essential prior to subsequent modeling and inspection to effectively suppress interference, recover structural features, and provide a reliable foundation for accurate point cloud reconstruction and key dimensional identification.

3.1. Low-Pass Filtering Point Cloud Denoising Algorithm

During three-dimensional (3D) laser scanning of large prefabricated box girders, the acquired point-cloud data are frequently contaminated by substantial noise. Such noise not only markedly increases the complexity of subsequent data processing and degrades overall data quality, but also impairs accurate extraction of critical feature points, which in turn can cause reconstructed point-cloud models to fail to meet the geometric-accuracy requirements of practical engineering applications. Therefore, targeted denoising of point clouds for large box girders is of considerable practical significance.

Based on the spatial distribution characteristics of noise points, they can be categorized into four types: drift points, isolated points, redundant points, and mixed points. Drift points are located far from the main structure, sparsely distributed in space, and often suspended above the point cloud. Isolated points are anomalous points situated away from dense regions of the point cloud; they form small clusters and exhibit distributions that differ markedly from surrounding points. Redundant points mainly refer to extraneous points acquired outside the scanning range or duplicate records. Mixed points are distributed around the periphery of the target object; they are sparse and difficult to distinguish from genuine structural elements. For the first three types of noise, open-source software such as Cloud Compare can be employed for screening and removal through multi-view visualization and manual interaction, for example, eliminating non-target point clouds

 doi:10.20944/preprints202605.0620.v1

corresponding to embedded reinforcement on box-girder sides or temporarily placed objects within the structure. However, because mixed points exhibit spatial distributions similar to those of target points and are therefore difficult to identify, manual processing is not only time-consuming and labor-intensive but also prone to the erroneous removal of valid point-cloud data, which in turn degrades the completeness and accuracy of the reconstructed surface models.

To address this, we propose an automated denoising strategy grounded in the principle of low-pass filtering. The algorithm traverses the point cloud and, for each target point, selects either a preset number of nearest neighbors or the neighboring points within a specified radius r, and fits a local plane to that neighborhood. A maximum error threshold w_r is introduced and the mean projection distance d_m of the neighborhood points onto the fitted plane is computed; if d_m exceeds w_r, the target point is classified as noise and removed. As shown in Figure 2, the resulting comparison illustrates the point-cloud denoising after removal of the various noise types. By using the neighborhood plane-projection error as the primary criterion, the method achieves precise identification of noise points while avoiding the loss of valid points associated with manual cleaning, thereby preserving the geometric integrity of the box-girder main structure. Furthermore, the automated workflow increases denoising efficiency by a factor of 3–5 compared with manual interactive deletion, making it well suited to large-scale engineering point-cloud processing.

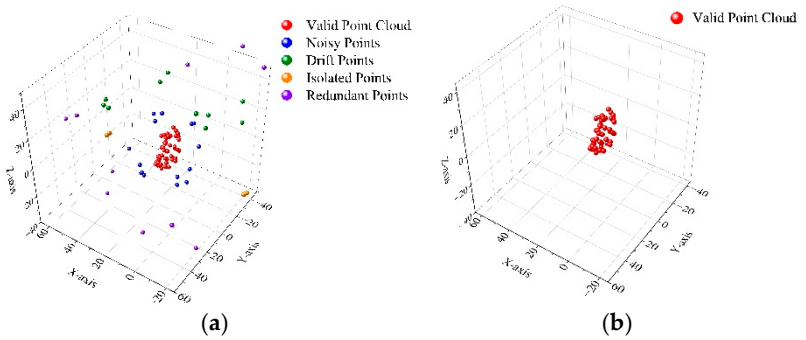

Figure 2. Denoising Comparison Diagram (a) Before Point Cloud Denoising (b) After Point Cloud Denoising.

3.2. Sequential Registration Point Cloud Stitching Algorithm

Due to the geometric configuration and large spatial scale of prefabricated high-speed railway box girders, three-dimensional laser scanning from a single station cannot fully capture all surfaces; therefore, multiple scanning stations must be deployed to acquire a complete, global point cloud. Data from each station are referenced to a local coordinate system centered on that scan, which leads to inconsistent coordinate frames across stations. To ensure spatial consistency of the assembled point cloud, a spatial-datum unification algorithm is applied to normalize the point-cloud datasets from all stations [21]. Through inter-station coordinate transformation and registration, a complete point-cloud model covering the entire box girder is constructed to satisfy the engineering requirements for subsequent inspection and analysis. The basic principle is illustrated in Figure 3.

 doi:10.20944/preprints202605.0620.v1

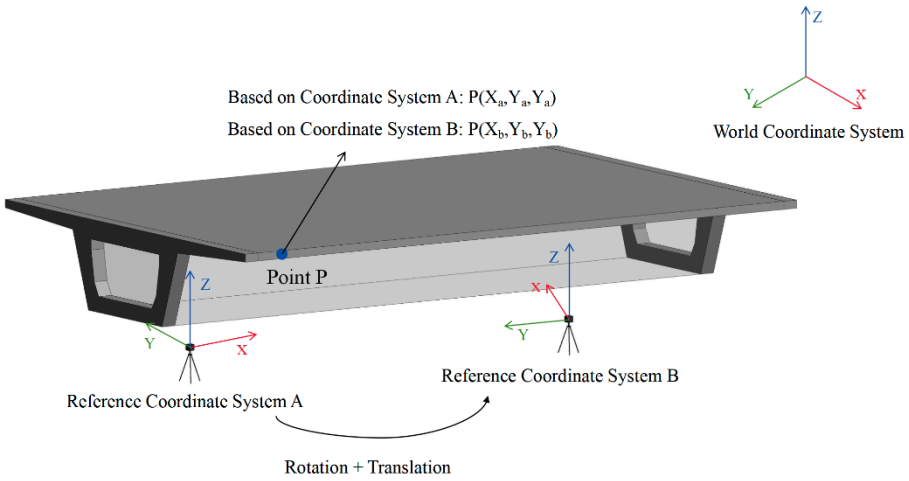

Figure 3. Point Cloud Stitching Principle.

As shown in Figure 3, the two scanning stations are defined in different local coordinate systems. Taking point P as an example, let its coordinates in station 1 and station 2 be (XA,,YA,ZA) and (XB,YB,ZB), respectively. The coordinate transformation can then be expressed as:

$$R = \begin{bmatrix} \cos\alpha & -\sin\alpha & 0 \\ \sin\alpha & \cos\alpha & 0 \\ 0 & 0 & 1 \end{bmatrix} \begin{bmatrix} \cos\beta & 0 & -\sin\beta \\ 0 & 1 & 0 \\ \sin\beta & 0 & \cos\beta \end{bmatrix} \begin{bmatrix} 1 & 0 & 0 \\ 0 & \cos\gamma & -\sin\gamma \\ 0 & \sin\gamma & \cos\gamma \end{bmatrix} \tag{1}$$

$$T = \begin{bmatrix} t_x \\ t_y \\ t_z \end{bmatrix} \tag{2}$$

In the above expression, α , β , γ denote rotation angles about the x ,y , and z, respectively, while t_x , t_y, t_z denote translations along the x , y , and z directions.

In this study, a sequential registration strategy was adopted to perform station-by-station merging of point clouds acquired from adjacent stations located at end faces, chamfers and similar positions. Given the high overlap between neighbouring scans and the pronounced geometric features of the box-girder edges, automated registration implemented in commercial point-cloud software (Cloud Compare) is appropriate: local feature descriptors are extracted from each station's point cloud, initial transformation parameters are obtained via feature matching to achieve a coarse alignment, and a subsequent bundle-adjustment step is applied to globally optimize registration errors, thereby improving alignment accuracy and overall consistency. This approach obviates bulk import of all point-cloud data and thus substantially reduces memory usage and computational load. Figure 4 presents the resultant integrated point cloud of the prefabricated concrete box girder obtained by stitching scans from different station angles.

 doi:10.20944/preprints202605.0620.v1

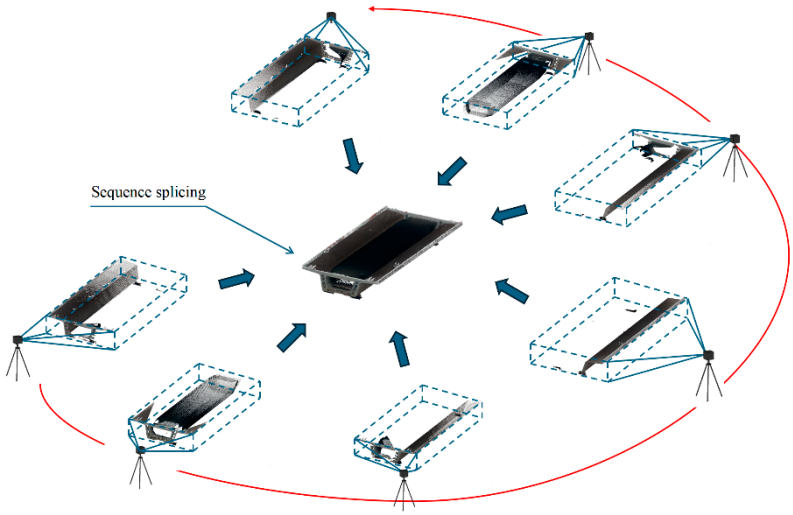

Figure 4. Point Cloud Stitching Diagram.

3.3. Multimodal Point Cloud Simplification Technology

As a representative large-scale precast concrete element, prefabricated box girders may extend longitudinally for tens of metres, and their three-dimensional laser-scanned point clouds are typically acquired at millimetre-level sampling density, yielding extremely large raw datasets. The coexistence of high-curvature sharp edges, localized fine-scale features and extensive planar regions on the box-girder surface produces pronounced spatial non-uniformity: complex curved regions are densely sampled while planar areas are comparatively sparse. In addition, the scanning process frequently generates outliers and redundant points caused by repeated structural elements, further exacerbating data irregularity. Direct processing of such raw point clouds therefore encounters dual bottlenecks of limited storage capacity and poor computational efficiency. Consequently, achieving an efficient data-reduction scheme that preserves critical geometric features is a necessary prerequisite for subsequent modelling and dimensional inspection.

Numerous point-cloud simplification methods have been developed, most of which are centred on geometric features such as inter-point distance, surface normals and curvature. In general, these methods can be classified into two main categories: mesh-based compression approaches and point-cloud-based compression approaches [22]. Considering the characteristics of prefabricated box-girder point clouds in terms of scale, density and spatial distribution, and aiming to preserve geometric fidelity while maintaining computational efficiency, this study proposes a multimodal point-cloud optimisation technique for efficient box-girder point-cloud reduction. The proposed technique integrates multi-scale voxel filtering with a curvature-sensitive enhancement strategy to perform down-sampling within a multi-dimensional data-processing framework. Specifically, a voxel-filtering method is first employed for coarse compression by partitioning the scanning space into regular cubic grids of a prescribed size and performing preliminary down-sampling within each grid. When the voxel edge length v is set to 5 mm, the three-dimensional space is divided into cubic cells with 5 mm edges, and all points within each cell are replaced by their centroid P , such that:

$$P = \left(\frac{1}{N}\sum_{i=1}^{n} x_i, \frac{1}{N}\sum_{i=1}^{n} y_i, \frac{1}{N}\sum_{i=1}^{n} z_i\right) \tag{3}$$

In this expression, N denotes the number of points within a voxel, and x_i, y_i, z_i represent the three-dimensional coordinates of the i-th point inside the voxel.

The above approach markedly reduces data volume while preserving the overall geometric shape: a 5 mm voxel resolution retains macroscopic dimensional fidelity (e.g., web thickness) while alleviating redundancy in planar regions.

 doi:10.20944/preprints202605.0620.v1

After the coarse compression effected by voxel filtering, a curvature-sensitive enhancement strategy is applied for fine-scale optimization. This strategy first computes local curvature using a covariance-matrix method, and defines a scalar Cλ to characterise curvature variation at each point. The algorithm then iterates over the preliminarily sampled points p and evaluates the corresponding Cλ for each. For a given point p, the neighbouring point set is searched within a radius r, and the covariance matrix Cov of that neighbourhood is constructed as:

$$Cov = \frac{1}{k}\sum_{i=1}^{k}(p_i - P)(p_i - P)^T \tag{4}$$

In this expression, P denotes the centroid of the neighbourhood points, and pi represents the coordinate vector of the i-th point within the neighbourhood.

Eigenvalue decomposition is then performed on the covariance matrix Cov, yielding eigenvalues λ1≥λ2≥λ3≥0, based on which the curvature descriptor Cλ is subsequently computed as:

$$C_\lambda = \frac{\lambda_3}{\lambda_1 + \lambda_2 + \lambda_3} \tag{5}$$

Finally, high-curvature points are selected according to a predefined curvature threshold to preserve feature-rich regions, thereby completing the point-cloud simplification process. The resulting effect is illustrated in Figure 5.

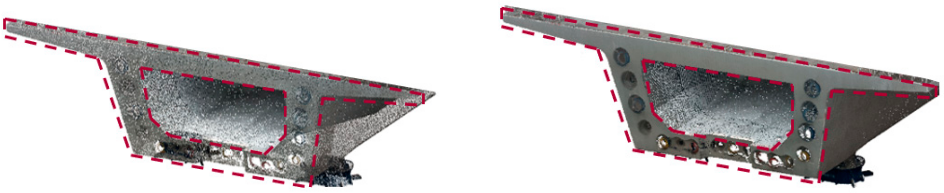

(**a**) (**b**)

Figure 5. Point Cloud Simplification Effect Diagram:(a) Before Point Cloud Simplification;(b) After Point Cloud Simplification.

4. Point Cloud Model Reconstruction Method for Large-Scale Box Girders

Owing to their large spans, thin walls and complex curved geometries, box girders generate laser-scanned point clouds that contain numerous edge-contour points, convex–concave transition surfaces and corner (curvature-discontinuity) points. These regions exhibit pronounced variations in surface normals that contrast sharply with smoothly curved areas and therefore provide a reliable basis for extracting salient geometric features and identifying key structural elements such as feature surfaces and feature lines. At the same time, the scanning environment in prefabrication yards is challenging: occlusion by supports, specular reflection from concrete surfaces, and the limited field of view and ranging capability of scanners commonly cause missing data in critical regions (for example, the bottom slab), which in turn induces geometric distortions in subsequent modelling such as surface discontinuities and blunting of sharp feature edges. Accordingly, there is an urgent need to develop reconstruction methods tailored to box-girder point-cloud characteristics — ad-vancing topology-aware connectivity, salient-feature detection and local data-completion tech-niques — to provide robust geometric models for subsequent high-precision dimensional inspec-tion.

4.1. Box Girder Point Cloud Feature Recognition Algorithm

During box-girder point-cloud processing, the raw data consist solely of discrete three-dimensional coordinates and colour attributes, without explicit topological relationships among points. This absence of topology not only constrains the efficiency of geometric-feature extraction but also increases the computational complexity of subsequent tasks such as surface reconstruction. To address these issues, we propose a combined approach that integrates neighbourhood-based topological modelling with multi-dimensional geometric-feature enhancement. By constructing

 doi:10.20944/preprints202605.0620.v1

neighbourhood relationships within the point cloud, the method establishes an explicit topological structure and leverages local geometric descriptors to enhance salient features.

In this study, a K-NN algorithm is employed to determine whether a point Pi is a boundary point. The decision criterion is based on the angle between directed line segments formed by Pi and its neighbouring points. This angle is compared with a predefined angular threshold: if the angle exceeds the threshold, Pi is classified as a boundary point; otherwise, it is regarded as an interior point. A schematic illustration of this principle is shown in Figure 6.

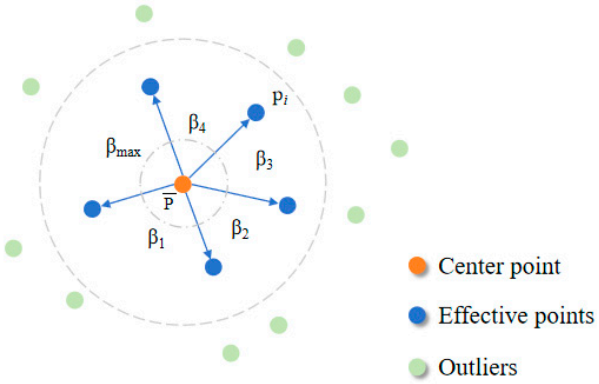

Figure 6. K-NN Relationship Model Diagram.

For boundary regions of the box-girder point cloud characterized by pronounced curvature discontinuities, PCA is further introduced to integrate normal-vector computation with curvature estimation, enabling accurate boundary identification. The core idea is to recast the estimation of the normal vector at a target point P as the problem of determining the normal of its local tangent plane. Specifically, a K-NN search is employed to select the neighbourhood point set N={ni|ni∈N}，i=1,2，…，k, where k denotes the number of neighbouring points. The centroid of the neighbourhood, $\bar{p}$, is then computed as:

$$\bar{p} = \frac{1}{k}\sum_{i=1}^{k} p_i \tag{6}$$

The normal vector of the least-squares fitted surface is computed according to the following expression:

$$\min_{\eta} = \sum_{i=1}^{k} \| (p_i - \bar{p}) \cdot \vec{n} \| \tag{7}$$

In this expression, $\vec{n}$ denotes the normal vector of the fitted plane.

The minimization above is equivalent to solving an eigenvalue problem for the covariance matrix Cov; specifically, the normal vector at the target point is given by the eigenvector associated with the smallest eigenvalue of Cov:

$$Cov = \sum_{i=1}^{k} (p_i - \bar{p})(p_i - \bar{p})^T \tag{8}$$

Eigenvalue decomposition is performed on the covariance matrix, yielding eigenvalues $\lambda 1$,$\lambda 2$,and $\lambda 3$ together with their corresponding eigenvectors v1 , v2, and v3.

The normals obtained from PCA are sign-ambiguous: if v is a principal direction then -v is equally valid, since both represent the direction of maximum variance. However, eigenvectors of the

 doi:10.20944/preprints202605.0620.v1

covariance matrix Cov carry no inherent positive or negative orientation and therefore must be reoriented with respect to the sensor (viewpoint) direction. This reorientation can be expressed as:

$$\vec{n} = \begin{cases} n_i & n_i \cdot (v_p - q) > 0 \\ -n_i & else \end{cases} \tag{9}$$

In this expression, v p denotes the viewpoint, and q represents the sampled point.

The curvature ϕ is then computed as the ratio of the smallest eigenvalue to the sum of all eigenvalues, expressed as:

$$\phi = \frac{\lambda_3}{\lambda_1 + \lambda_2 + \lambda_3} \tag{10}$$

The above multi-scale approach effectively captures edge details across scales and consequently improves boundary accuracy; however, it also introduces additional iterations and redundant storage, which increase computational time and resource consumption. To improve efficiency, a detection-window parameter is provisionally set to 10 and the point cloud is traversed: points whose curvature values exceed the prescribed threshold are tentatively classified as boundary points. In the subsequent, coarser-scale pass a plane-fitting–based curvature estimator is used, and points previously classified as non-boundary are excluded from further computation. The boundary detection results for the box-girder end face are shown in Figure 7.

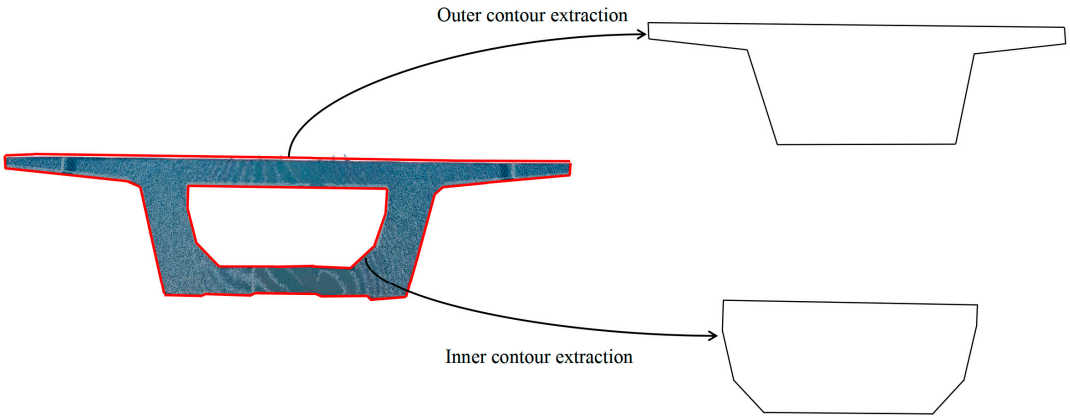

Figure 7. Box Girder End Face Boundary Extraction.

4.2. Filling of Missing Point Clouds for Box Girders

During field acquisition of point clouds in the storage area of prefabrication yards, data incompleteness is particularly pronounced, primarily due to the combined constraints of scanning geometry and instrument performance. On the one hand, large on-site metal fixtures such as supports and beam-storage racks induce self-occlusion, and—when coupled with the high specularity of concrete surfaces—these effects exacerbate scanning blind spots. On the other hand, the limited field of view and maximum ranging capability of laser scanners impede complete capture of the full-surface geometry of wide-span elements such as the bottom slab, resulting in widespread missing data. Representative local patterns of such data loss are shown in Figure 8.

This study employs B-spline curve fitting, least-squares optimisation and the iterative closest point (ICP) algorithm to fill and repair the box-girder soffit (underside) and local voids in incomplete point clouds. The proposed reconstruction restores the complete geometry of the box-girder point cloud, thereby facilitating the extraction of refined geometric measurements and providing a reliable geometric model for subsequent dimensional inspection.

 doi:10.20944/preprints202605.0620.v1

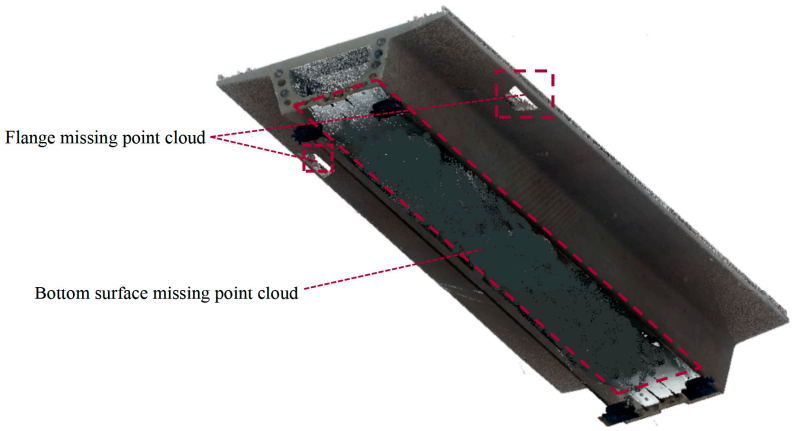

Figure 8. Wing Flange Side Missing Point Cloud.

4.2.1. Filling of Box Girder Bottom Surface

In precast box-girder construction, prestressing (tensioning) is employed to improve crack resistance and stiffness, but the induced forces can produce reverse-camber deformation so that the deck and soffit exhibit slight upward camber. Consequently, filling missing point-cloud regions must reproduce the true deformed surface rather than substituting simple planar patches. Moreover, chamfered transitions are commonly provided at the junction between soffit and web to mitigate stress concentrations, and the reconstruction must preserve smooth geometric transitions in these areas. To meet these requirements, the soffit-repair procedure is as follows. First, the covariance matrix of the point cloud at the soffit–web interface is computed and high-curvature feature points are extracted using a curvature threshold of 0.1; the chamfer region is then segmented by clustering high-curvature points with an additional constraint on normal-vector angular difference, and a B-spline curve is fitted to obtain the chamfer boundary contour. Second, a chamfer surface is generated along the intersection line using the design chamfer radius R=50mm, and the overall soffit is reconstructed by a moving least-squares (MLS) surface-fitting step to ensure a smooth junction between the chamfer and the main soffit surface. Finally, during the connection-stage refinement, the generated chamfer surface is fused with the retained original point cloud and MLS-based local smoothing is applied to the stitching boundary; sampling along the chamfer edge is densified at the design radius to improve the localization accuracy of geometric features.

Following the above procedures, the reconstructed soffit surface closely conforms to the actual deformation of the box girder induced by prestressing while effectively mitigating stress-concentration risks at the chamfered transitions. The repair quality can be directly validated by three-dimensional point-cloud visualization; the filled underside of the girder is shown in Figure 9.

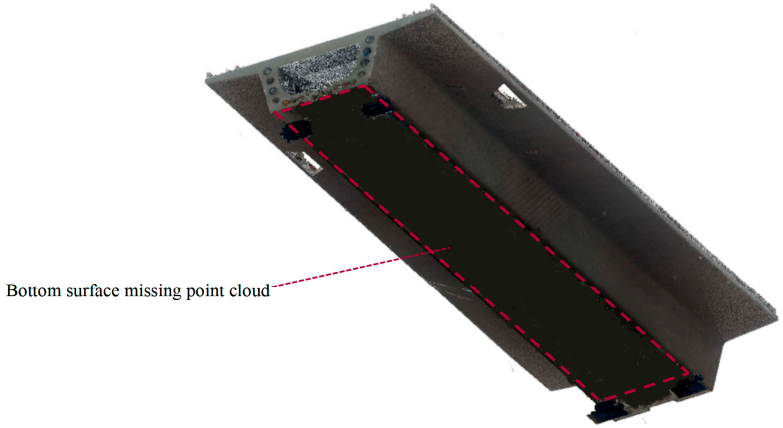

 doi:10.20944/preprints202605.0620.v1

Figure 9. Box Girder Bottom Surface Filling.

4.2.2. Wing Flange Void Repair

To address point-cloud data loss caused by embedded reinforcement in railway box-girder flanges, this study proposes a repair strategy that integrates geometric symmetry with surface reconstruction, with particular emphasis on restoring single-sided missing regions formed by occlusion on concrete surfaces. First, PCA is used to extract the longitudinal principal direction of the box girder: the covariance matrix of the point cloud is computed, and the eigenvector corresponding to the largest eigenvalue is taken as the normal vector of the symmetry plane, enabling high-precision localization of the flange mid-symmetry plane. Next, this symmetry plane is used to perform a rigid transformation of the point cloud on the intact flange side—specifically, a mir-ror-mapping operation about the symmetry plane is applied to generate an initial filled point cloud for the missing side. This process, implemented via coordinate-system rotation and translation, strictly preserves geometric symmetry correspondence. To address potential geometric discontinu-ities between the mirrored surface and the original surface, feature control points P are introduced in the boundary region, and a cubic B-spline surface is employed to construct a transition zone. Owing to the local control properties of B-spline surfaces, smooth geometric transitions are achieved, avoiding abrupt changes between the repaired region and the original structure. Finally, to further improve reconstruction accuracy, an iterative closest point (ICP) algorithm is applied to optimize feature matching between the original and mirrored boundaries. Using point-to-surface distance as the metric, the rotation and translation parameters of the rigid transformation matrix T are itera-tively refined until geometric consistency between the transition surface and the original structure is satisfied. By imposing symmetry constraints, the proposed method significantly reduces computa-tional complexity, and in combination with B-spline surface optimization and ICP-based fine ad-justment, effectively enhances the geometric accuracy and continuity of the repair results. This approach successfully resolves flange point-cloud loss caused by occlusion from embedded rein-forcement. The reconstructed overall point-cloud model of the box girder is shown in Figure 10.

Figure 10. Complete Box Girder Point Cloud Model.

5. Feature-Driven Dimensional Inspection Method for Box Girders

To mitigate the high computational complexity and low feature-extraction efficiency associated with processing massive point-cloud datasets of large-scale beams, practitioners commonly adopt a geometry-constrained, hierarchical slicing strategy to streamline the workflow [23,24]. In this study, and following the key measurement locations prescribed by beam-dimension inspection standards, cutting planes are placed along the beam's longitudinal axis at fixed intervals (end section, L/5、2L/5、3L/5、4L/5), partitioning the raw point cloud into multiple geometrically coherent subregions. Each subregion corresponds to the local structure of a specific beam segment; within these segments the point-density distribution is more uniform and noise interference is effectively

 doi:10.20944/preprints202605.0620.v1

suppressed, thereby providing a more stable data foundation for subsequent feature extraction and dimensional computation.

By orthogonally projecting the point-cloud data on both sides of each cutting plane onto a reference plane, the three-dimensional point set is reduced to a two-dimensional representation, substantially lowering data volume while preserving key geometric features. This hierarchical slicing strategy not only aligns with the beam's structural-mechanical characteristics—particularly the stress distribution at web–flange junctions—but also mitigates numerical singularities in global computations, thereby providing a more reliable data foundation for subsequent feature-line extraction and deformation analysis. A schematic of the box-girder point-cloud segmentation model is shown in Figure 11.

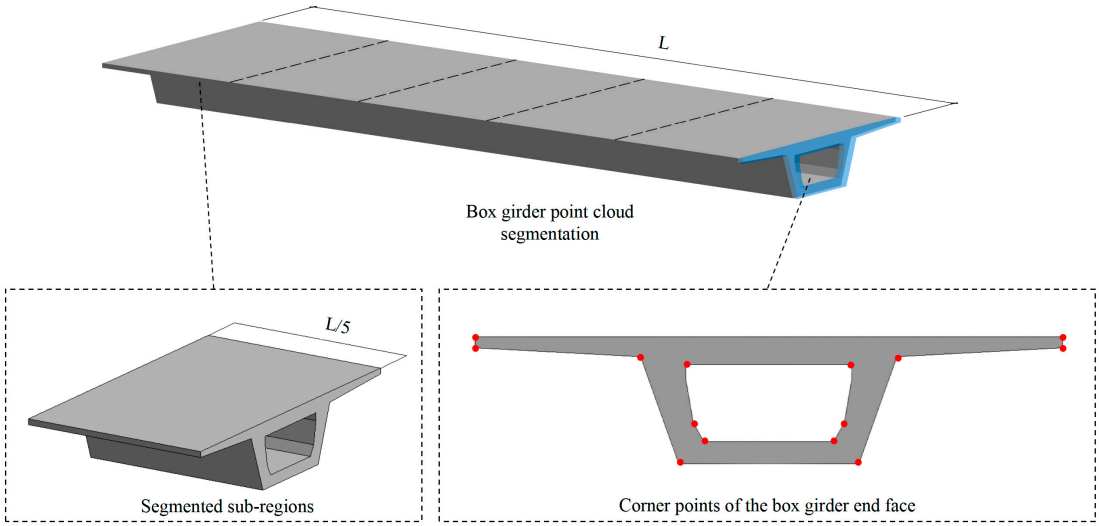

Figure 11. Box Girder Point Cloud Segmentation-Corner Point Extraction Model Diagram.

5.1. Box Girder Feature Corner Points

Prefabricated high-speed-rail box girders are characterised by hollow cross-sections and sharply defined edges. From the viewpoint of 3D point-cloud feature analysis, the corner points at the beam ends exhibit several engineering-relevant properties. First, they show strong geometric correlation: these points concentrate along the intersection lines of primary load-bearing elements (web–flange and crossbeam–web junctions), and their spatial coordinates directly reflect the geometric convergence of the cross-section. Second, they possess excellent topological stability: during reverse-camber deformation induced by prestressing, displacements of the corner points display a pronounced linear relationship with overall profile deviations, making them sensitive indicators for deformation monitoring. Third, they offer superior detection robustness: compared with conventional total-station surveys that are prone to occlusion, corner points—being local extrema of geometric curvature—can be located with high precision by exploiting point-cloud density and local geometric cues.

5.2. Box Girder Feature Corner Point Recognition Method

After sectioning the beam point cloud, we further reduce data volume and precisely extract geometric features by projecting each slice onto a reference plane to obtain two-dimensional contour point sets. This dimensionality-reduction step substantially lowers data complexity while efficiently capturing component boundary features, thereby laying the foundation for accurate corner-point extraction required for subsequent dimensional inspection. Informed by the end-geometry of the box

 doi:10.20944/preprints202605.0620.v1

girder, the feature corner points to be extracted are classified into two types: (1) intersections of two or more edge lines, and (2) junctions where three planes or surfaces meet. Together, these two classes constitute the geometric landmarks of the component's critical locations.

Given the general applicability of the CSS corner detector to contour analysis—which, via edge detection or multi-scale curvature computation, is robust to rotation, translation and noise and can stably identify curvature extrema on contours of arbitrary shape—we adopt this algorithm for end-face corner extraction. In practice, the CSS algorithm is applied to the previously extracted edge-line data of the beam end; multi-scale curvature analysis is then used to select curvature extrema that satisfy the prescribed constraints, thereby extracting the key corner points that represent the end geometry of the box girder. The computational procedure is as follows: first, acquire the boundary point cloud of the box-girder end and reconstruct the edge line, converting the boundary into a continuous curve parameterized by arc length s, (x(s),y(s)); second, smooth the curve on the reference plane by applying Gaussian filters at multiple scales σ, chosen to cover both the largest and smallest corner features, and separately filter the x- and y-components to obtain X（s，σ）:

$$X(s,\sigma)=x(s)\cdot G(s,\sigma) \tag{11}$$

$$Y(s,\sigma)=y(s)\cdot G(s,\sigma) \tag{12}$$

For a given parametric vector representation of a planar curve, the curvature is computed as follows:

$$k(s)=\frac{\dot{x}(s)\ddot{y}(s)-\ddot{x}(s)\dot{y}(s)}{(\dot{x}^2(s)+\dot{y}^2(s))^{\frac{3}{2}}} \tag{13}$$

In the expression, $\dot{x}$ and $\dot{y}$ denote first derivatives, $\ddot{x}$、and $\ddot{y}$ denote second derivatives, and s denotes the arc length between two points along the curve.

$$s=\int_{P_1}^{P_2}\sqrt{\dot{x}^2(s)+\dot{y}^2(s)}dt \tag{14}$$

When the curve is parameterized by s, that is, $\dot{x}^2(s)+\dot{y}^2(s)=1$, the curvature in the CSS framework for an arc-length parameterized planar curve can be expressed as:

$$k(s)=\dot{X}(s)\ddot{Y}(s)-\ddot{X}(s)\dot{Y}(s) \tag{15}$$

For curvature maxima across multiple scales, curvature extrema with small absolute values are first identified and discarded. The remaining curvature maxima are then screened: a point that is detected in adjacent scales is classified as a stable feature. Spatially proximate detections are merged via clustering. By referencing the end-geometry and design drawings of the box girder, corner points that do not correspond to design-intended locations are removed; the retained corner points are overlaid on the original imagery and their validity is confirmed through interactive human–computer verification. The corner-point detection results for the box-girder end face are shown in Figure 1.

6. Rationality Verification and Engineering Application of Large-Scale Prefabricated Box Girder Inspection Methods

6.1. Project Overview

This study investigates 31.5-m post-tensioned prefabricated box girders used in the Xiong'an–Xinzhou high-speed railway. In storage yards, these girders experience dynamic changes in alignment due to prestressing forces and concrete creep, making direct modelling based on design drawings impractical and necessitating in situ geometric dimension inspection. Measurements were conducted at the Wutai beam fabrication yard of the Xiong'an–Xinzhou high-speed railway; the inspected girders are shown in Figure 12. A total of nine prefabricated girders were randomly

 doi:10.20944/preprints202605.0620.v1

selected for appearance-dimension inspection, labelled WT-01 to WT-09. According to Prefabricated Post-tensioned Prestressed Concrete Simply Supported Beams for High-speed Railways (GB/T 37439-2019) and related bridge and culvert acceptance standards, finished-beam acceptance requires measurements of overall beam length, deck width, web thickness, beam depth, and top- and bottom-slab thicknesses. The design values and allowable tolerances for each inspection item are listed in Table 1.

Table 1. Design values and allowable tolerances for inspection items.

No.	Item	Design value (mm)	Allowable tolerance (mm)
1	Span	31,500	±20
2	Overall beam length	32,600	±20
3	Deck (bridge) width	12,600	+10,−10
4	Web (wall) thickness	900	+10,−5
5	Beam depth (height)	3,015	+10,−5
6	Top slab thickness	555	+10,−0
7	Bottom slab (soffit) thickness	600	+10,−0

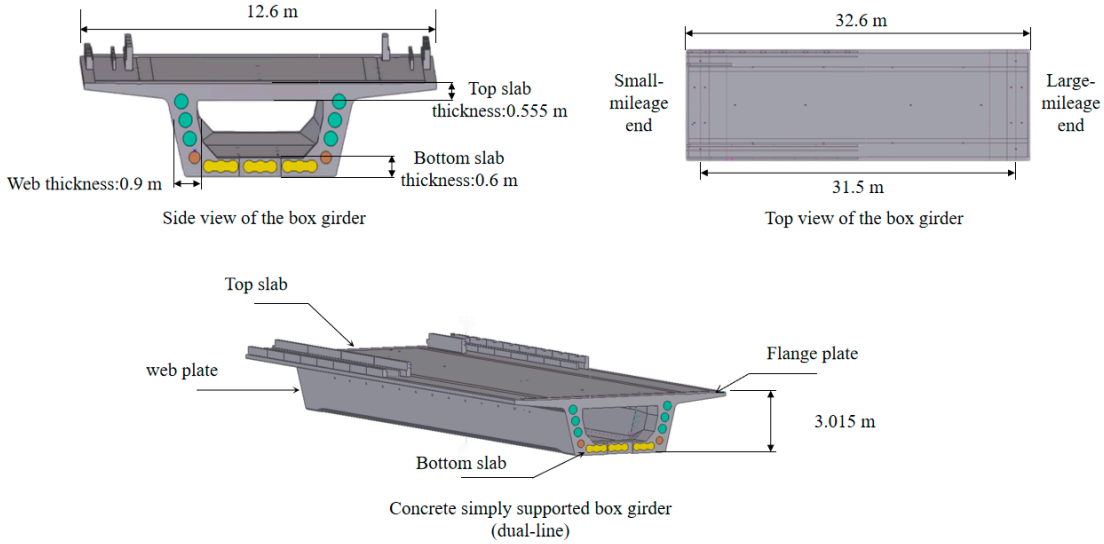

Figure 12. Box Girder Inspection Information.

6.2. Scanner Selection and Station Layout

6.2.1. Equipment Selection

In large-scale prefabricated box-girder construction, member lengths commonly reach 24 m, 32 m and even up to 40 m, imposing stringent requirements for high-precision, high-efficiency 3D data acquisition in storage yards. In practice, however, the completeness, accuracy and reliability of point-cloud data are substantially challenged by factors such as scanner range, incidence angle, scanner-station layout and prevailing climatic conditions. Consequently, equipment selection must strike a balance among scanning coverage, compatibility with target dimensions and project budget to ensure both the technical feasibility and cost-effectiveness of the chosen solution.

After a systematic evaluation, this study selected the portable SPL-1500 3D laser scanner for point-cloud data acquisition. This device offers efficient scanning capabilities for medium and long-range distances, with a scanning range of 1.5 m to 1500 m and a measurement speed of up to 2 million points per second. It features a highly integrated hardware design, with an overall weight of only 4.85 kg and built-in dual-axis compensation, enabling quick operation without the need for leveling. Additionally, the scanner is equipped with dual 12.3-megapixel high-resolution cameras for fast color rendering of the real scene. It also integrates multiple sensors, including GNSS, an electronic compass,

 doi:10.20944/preprints202605.0620.v1

altimeter, and thermometer, for real-time monitoring of the device's status. The scanner provides multimodal hardware interfaces and standardized communication protocols, allowing for easy integration with various application systems, offering excellent compatibility and effectively adapting to the complex construction environment of beam yards. The selected scanner is shown in Figure 13.

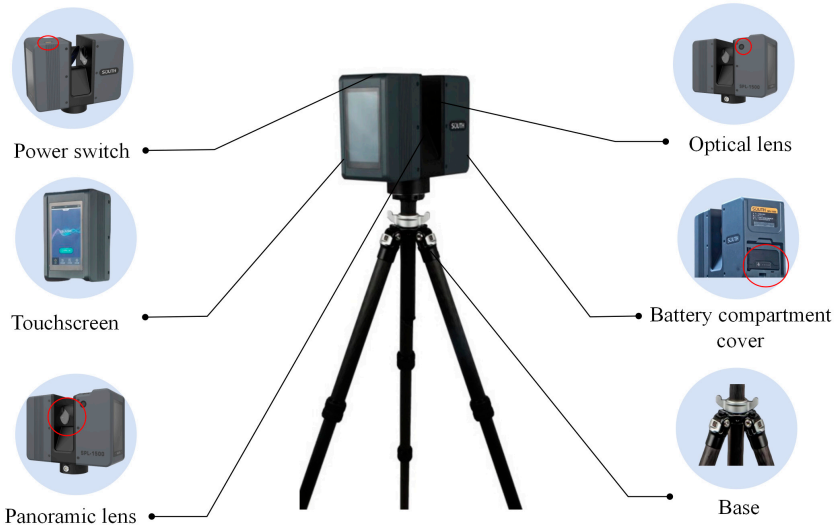

Figure 13. SPL-1500 3D Laser Scanner.

6.2.2. Station Layout

Before conducting 3D laser scanning in the storage area for prefabricated box girders, a comprehensive survey of the storage yard environment must first be conducted. The spatial location of the scanning stations and the distance from the stations to the target beams should be scientifically planned, taking into account the geometry, dimensional parameters of the prefabricated beams, as well as the technical specifications of the scanner, including range and measurement accuracy. This ensures that the station layout fully covers key feature areas on both the end faces and sides of the beams while effectively avoiding scanning blind spots or redundancy caused by excessive overlap of point-cloud data.

Traditional 3D scanning station deployment schemes typically rely on strategically placing common targets, which serve as a coordinate transfer reference between multiple stations. Through precise point-cloud registration and stitching, a complete 3D model is generated. These methods can generally be categorized into two types: tail-to-tail registration for two stations and global registration for multiple stations [25,26]. With the ongoing iteration of point-cloud registration algorithms, continuous improvements in hardware performance, and the increasing demand for efficiency and automation in complex engineering environments, 3D scanning technology has evolved to include a target-free scanning mode. This method eliminates the need for physical targets and instead uses algorithms to match 3D data features in overlapping areas between multiple stations, aligning the spatial coordinates directly. For prefabricated box girders, which have prominent edges and regular geometric features, the data processing process requires only the extraction and matching of corresponding feature points between different stations to complete the stitching. Compared with traditional target-based methods, target-free scanning eliminates the need for control points or targets, significantly improving field inspection efficiency. However, this method has stricter requirements for the extent of overlapping areas between scanning stations, with a recommended overlap of 20%–30% to ensure the accuracy of registration meets engineering needs.

 doi:10.20944/preprints202605.0620.v1

To balance the efficiency and completeness of 3D laser scanning data acquisition, and to address the structural characteristics of the box girder as well as the need for compensating potential scanning blind spots, this study adopts a multi-view collaborative stationing strategy, setting up 11 stations in total. The specific station layout is shown in Figure 14. The station locations and their respective functions are as follows: 1) End region: Two stations are symmetrically placed approximately 4 meters from the beam ends to ensure complete capture of the end geometry and avoid blind spots caused by curvature discontinuities; 2) Side region: A station is placed at the mid-span cross-section of the beam, offset about 6 meters outward along the web centerline, effectively covering the complex curves at the web-flange junction and minimizing local occlusions from changes in web thickness; 3) Top slab region: A station is located on the longitudinal symmetry axis of the top slab, 4 meters from each end, using a downward scanning mode to capture high-resolution data of the slab's flatness and reinforcement features; 4) Interior of the box girder: An additional station is set at the mid-span cross-section to focus on capturing detailed features inside the box, such as the internal chamfer and diaphragms.

The point-cloud overlap between adjacent stations is maintained above 20% to ensure seamless stitching after data registration. For blind spots formed by the obstruction of the soffit due to supporting structures, surface fitting is applied to the overlapping areas of adjacent stations. This is combined with geometric constraints, such as the web edge lines and flange profiles, and optimized using the ICP algorithm to achieve high-precision data reconstruction for the missing regions.

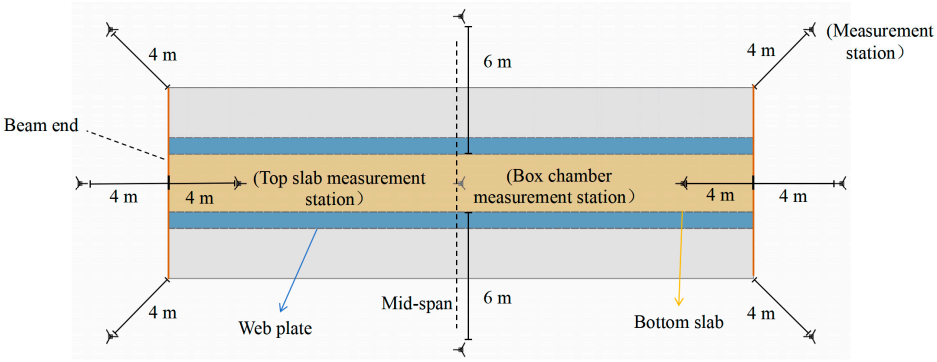

Figure 14. Scanning Station Layout.

6.3. Point Cloud Data Acquisition and Analysis

After completing the multi-view collaborative stationing plan and setting up the stations, 3D laser scanning of the beam is carried out. Since the raw point-cloud data from a single station typically exceeds 1.5 million points, the first step to enhance processing efficiency and accuracy is to use the open-source software Cloud Compare for interactive denoising. This process removes redundant point clouds outside the target beam's range and large noise clusters caused by environmental interference. Next, a low-pass filter is applied to eliminate outlier noise points, reducing the point-cloud data volume for a single beam. For segmented beam point clouds collected from multiple stations, a semi-automated stitching process is implemented based on a sequential registration algorithm, ultimately integrating the data into a complete point-cloud model that covers the entire beam.

Given the issue of excessive data volume in the stitched complete point cloud, coarse and fine compression processes are sequentially applied. Building on the contour extraction and feature calculation methods introduced in Sections 3 and 4, operations such as beam profile boundary extraction, missing point cloud completion, point cloud segmentation, and feature point extraction are performed in succession, enabling precise calculation of the various dimensional inspection parameters.

 doi:10.20944/preprints202605.0620.v1

5.3.1. Validation Experiment

To verify the practical effectiveness of the optimized station layout and point-cloud processing algorithm proposed in this study for the dimensional inspection of 32-meter prefabricated box girders, a comparative experiment was designed. Nine prefabricated box girders were tested using both 3D laser scanning and conventional manual measurement methods for three key dimensions: the left-end width of the deck long line, the width at the H-end, and the beam height. The traditional manual measurement method relies on tools such as a level and steel tape measure, following a set process to measure each girder individually, as shown in the comparison process in Figure 15. The 3D laser scanning method, on the other hand, generates a high-precision model of the entire beam using the aforementioned multi-view stationing and point-cloud processing workflow, followed by dimensional calculation. A comparison of the results from both methods is shown in Figure 16.

(**a**) (**b**)

Figure 15. Comparison of Detection Processes:(a) Manual Measurement Monitoring;(b) 3D Laser Scanning Monitoring.

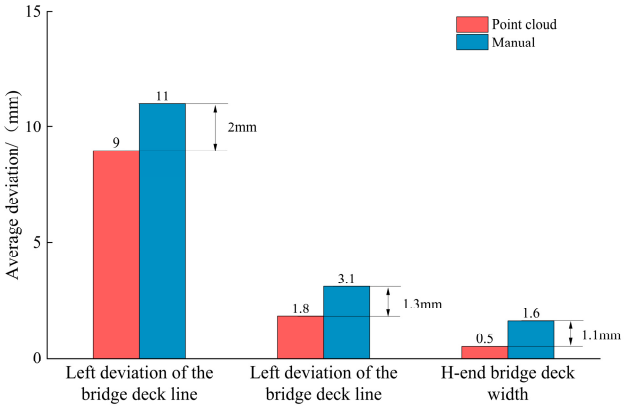

Figure 16. Comparison of Average Deviation Values.

As shown in Figure 16, this study compared the results of the 3D laser scanning method and traditional manual measurement for three key dimensions of the prefabricated box girder: the left-end width of the deck long line, the width at the H-end, and the beam height. The average absolute differences between the two methods were 2.0 mm, 1.3 mm, and 1.1 mm, respectively, with measurement errors for both methods being less than 1%. These results indicate that after the point cloud is processed with denoising, registration, compression, and feature extraction as described in this study, the geometric fidelity of the dimensional information is effectively preserved. This verifies that the point-cloud-based dimensional inspection method offers high measurement precision and reliability.

6.3.2. Beam Exterior Dimensional Accuracy Testing

 doi:10.20944/preprints202605.0620.v1

After processing the point-cloud data of the 9 girders, the beam number-deviation scatter plot shown in Figure 17 was generated. As can be seen from the Figure, the measurement deviations for certain exterior dimensions of the box girder—such as overall beam length, deck width, web thickness, beam height, top-slab thickness, and bottom-slab thickness—obtained using the 3D laser scanning technology all fall within the allowable tolerance limits specified in Table 1. This demonstrates that the method meets the predefined accuracy and reliability requirements for practical engineering inspections.

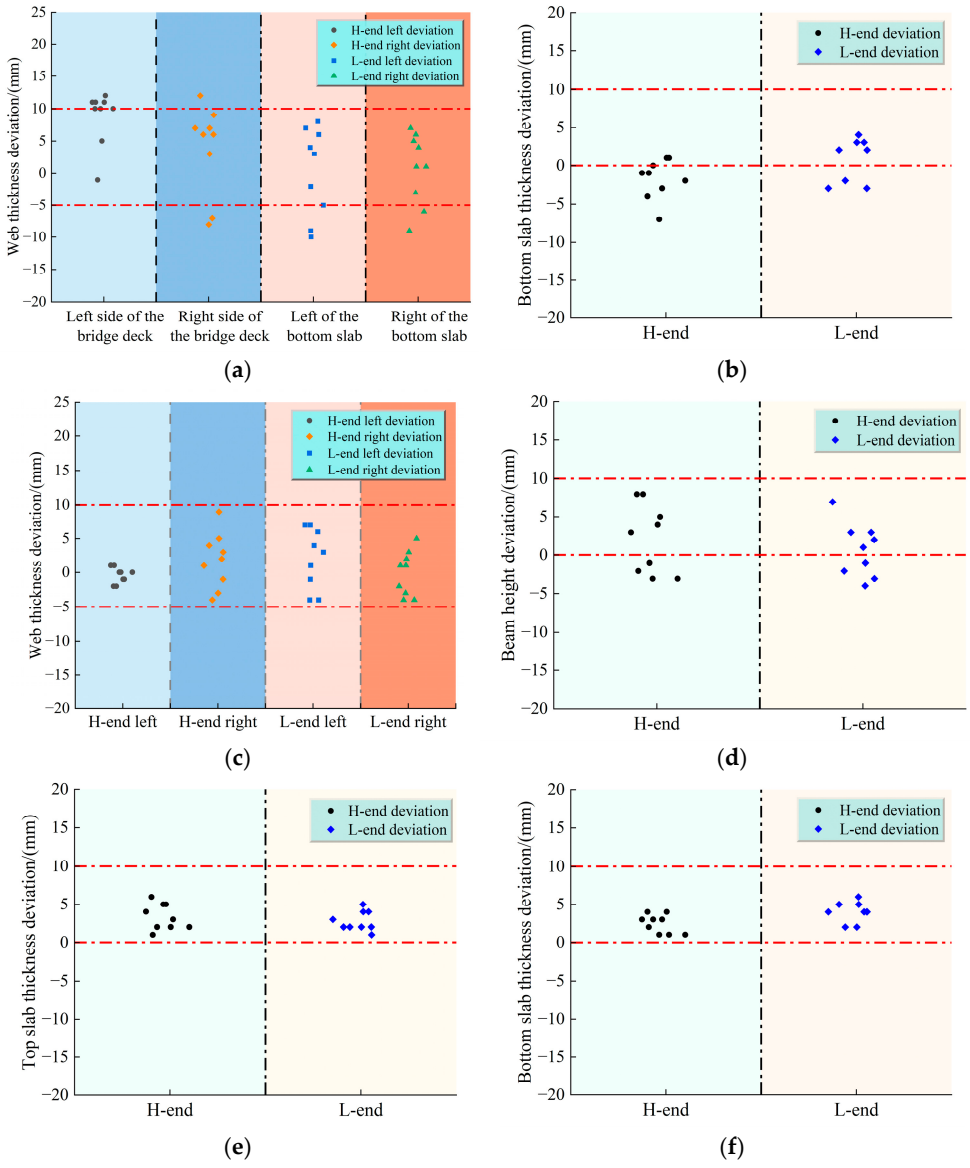

Figure 17. Detection Deviation:(a) Beam Number-Beam Length Deviation;(b) Beam Number-Deck Width Deviation;(c) Beam Number-Web Thickness Deviation(d) Beam Number-Beam Height Deviation;(e) Beam Number-Top Slab Thickness Deviation;(f) Beam Number - Bottom Slab Thickness.

7. Conclusions

This study addresses long-standing issues in the inspection of large-scale railway prefabricated box girders, such as reliance on manual contact measurements, low levels of automation, and inadequate result visualization. Leveraging the engineering practice at the Wutai beam fabrication yard of the Xiong'an–Xinzhou high-speed railway, an innovative, full-process non-contact inspection system has been developed. This system covers data acquisition, processing, reconstruction, and dimensional inspection.

 doi:10.20944/preprints202605.0620.v1

(1) In the data preprocessing stage, low-pass filtering, sequential registration, and multimodal point-cloud optimization techniques are applied to process the box-girder point cloud data. Combined with a curvature-adaptive downsampling strategy, this approach improves processing efficiency by 3 to 5 times while preserving key features, effectively addressing the issue of point-cloud redundancy in large-scale box girders.

(2) To address the challenges of structural complexity, scanning occlusion, and data incompleteness in large-scale box-girder point-cloud model reconstruction, a point-cloud reconstruction method is proposed that integrates topological relationship modeling with multi-scale feature enhancement. Through multi-scale feature enhancement, surface smoothing transitions, and data completion strategies, the geometric integrity of the model and the accuracy of dimensional inspection are significantly improved.

(3) A hierarchical slicing strategy guided by geometric constraints for large-scale railway prefabricated box girders is developed. The CSS algorithm is used to automatically identify eight key geometric features, and projection-based dimensionality reduction is employed to efficiently extract feature corner points.

(4) A comparative inspection of laser point clouds and traditional manual measurement methods was conducted in a real-world engineering context. The results demonstrate that the developed algorithm offers advantages in both speed and accuracy, meeting the precision requirements for large-scale prefabricated box girder structural inspection. In the experiments, the dimensional measurements of all girders complied with the design specifications and relevant standard limits.

The results of this study have been successfully applied to the finished-product inspection of prefabricated box girders at the Wutai beam fabrication yard of the Xiong'an–Xinzhou high-speed railway. This has facilitated the practical application of non-contact data acquisition technologies such as 3D laser scanning and automated analysis algorithms in the quality inspection of bridge engineering prefabricated components, demonstrating strong engineering adaptability and significant potential for widespread implementation.

Author Contributions: Zhang Zhiguo: Conceptualization, Data curation, Formal analysis, Funding acquisition, Investigation, Methodology. Dou shihao: Resources, Software, Supervision, Writing – original draft. Zhang Shaopeng: Supervision, Visualization. Chen kang:,Writing – review & editing.

Funding: This work has been supported by the Major Science and Technology Development Project of China State Railway Group Co., Ltd (K2023G004) and the Key Project of Scientific Research and Development Plan (N2023G080-A(JB)) of China State Railway Group Co., Ltd.

Informed Consent Statement: Written informed consent has been obtained from the patient(s) to publish this paper.

Data Availability Statement: The authors declare that they have no known competing financial interests or personal rela-tionships that could have appeared to influence the work reported in this paper.

Acknowledgments: This work has been supported by the Major Science and Technology Development Project of China State Railway Group Co., Ltd (K2023G004) and the Key Project of Scientific Research and Development Plan (N2023G080-A(JB)) of China State Railway Group Co., Ltd.

Conflicts of Interest: The authors declare no conflicts of interest.

References

1. R. Wong, J.L. Hao, P.X.W. Zou, The application of precast concrete technology in buildings and civil structures construction: Hong Kong experience, Sustainability and Innovation in-Management and Technology, Hong Kong, China, December 10–12Proceedings of the Second International Conference on Construction in the 21 st Century (CITC-II) 2003, pp. 629–634.

 doi:10.20944/preprints202605.0620.v1

2. L. Jaillon, C.S. Poon, Y.H. Chiang, Quantifying the waste reduction potential of using pre-fabrication in building construction in Hong Kong, Waste Manag. 29 (1) (2009) 309–320, http://dx.doi.org/10.1016/j.wasman.2008.02.015.
3. Han, X., Liu, W., Jiang, Z., et al. (2021). Practice of Intelligent Railway Precast Beam Yard. China Railway, (09), 73-78. DOI: 10.19549/j.issn.1001-683x.2021.09.073.
4. D. Wang, Y. Zhang, Y. Pan, B. Peng, H. Liu and R. Ma, "An Automated Inspection Method for the Steel Box Girder Bottom of Long-Span Bridges Based on Deep Learning," in IEEE Access, vol. 8, pp. 94010-94023, 2020, doi: 10.1109/ACCESS.2020.2994275.
5. Raj T, Hanim Hashim F, Baseri Huddin A, et al. A survey on LiDAR scanning mechanisms[J]. Electronics, 2020, 9(5): 741. M. Golparvar-Fard, J. Bohn, J. Teizer, S. Savarese, F. Peña-Mora, Evaluation of image-based modeling and laser scanning accuracy for emerging automated performance monitoring techniques, Autom. Constr. 20 (8) (2011) 1143–1155, http://dx.doi.org/10.1016/j.autcon.2011.04.016.
6. Qi, Y., Lin, P. (2025). Review on the Application of Point Cloud Technology in Civil Engi-neering. Engineering Mechanics, 1-23. [2025-10-24].
7. S. Han, H. Choe, S. Kim, et al., Automated and efficient method for extraction of tunnel cross sections using terrestrial laser scanned data, J. Comput. Civ. Eng. 27 (3)(2013) 274–281, http://dx.doi.org/10.1061/(ASCE)CP.1943-5487.0000211.
8. Zhou, Y., Wang, W., Luo, H. et al. Virtual pre-assembly for large steel structures based on BIM, PLP algorithm, and 3D measurement. Front. Eng. Manag. 6, 207–220 (2019).
9. Liu J , Zhang Q , Wu J ,et al.Dimensional accuracy and structural performance assessment of spatial structure components using 3D laser scanning[J].Automation in Construction, 2018, 96(DEC.):324-336.
10. Raibulet C , Fontana F A , Zanoni M .Model-Driven Reverse Engineering Approaches: A Systematic Literature Review[J].IEEE Access, 2017:1-1.DOI:10.1109/ACCESS.2017.2733518.
11. Durupt A , Remy S , Eynard G D & B .From a 3D point cloud to an engineering CAD model: a knowledge-product-based approach for reverse engineering[J].Virtual and Physical Proto-typing, 2008.DOI:10.1080/17452750802047917.
12. M.K. Kim, H. Sohn, C.C. Chang, Automated dimensional quality assessment ofprecast con-crete panels using terrestrial laser scanning, Autom. Constr. 45 (2014) 163–177, http://dx.doi.org/10.1016/j.autcon.2014.05.015.
13. Yang Y , Fang H , Fang Y ,et al.Three-dimensional point cloud data subtle feature extraction algorithm for laser scanning measurement of large-scale irregular surface in reverse engi-neering[J].Measurement, 2020, 151(000):11.DOI:10.1016/j.measurement.2019.107220.
14. Herráez, J., Martínez, J. C., Coll, E., Martín, M. T., & Rodríguez, J. (2016). 3D modeling by means of videogrammetry and laser scanners for reverse engineering. Measurement, 87, 216–227. https://doi.org/10.1016/j.measurement.2016.03.005
15. Song, J., Liu, H., Du, Y., et al. (2022). Automatic Reverse Modeling Method Based on 3D Laser Point Cloud of Concrete Combined Box Girder Defects. World Bridges, 50(1), 72-78.
16. WANG Qian, SOHN H, CHENG JC P. Development of high-accu-racy edge line estimation algorithms using terrestrial laser scanning[J].Automation in Construction, 2019,101:59-71.
17. Zhao W, Jiang Y, Liu Y, Shu J. Automated recognition and measurement based on three-dimensional point clouds to connect precast concrete components[J]. Automation in Construction,2022,133:104000.
18. Wu, W., Wang, X., Liu, H., et al. (2023). Research on Appearance Size Detection Method for Prefabricated Concrete Box Girder Based on Laser Point Cloud. Bridge Construction, 53(04), 25-32. DOI: 10.20051/j.issn.1003-4722.2023.04.004.
19. WANG C, CHO Y K, KIM C. Automatic BIM Component Extraction from Point Clouds of Existing Buildings for Sustainability Applications[J]. Automation in Construction, 2015, 56: 1-13.
20. Shen Y H. Point Cloud Modeling Based on Compactly Supported Radial Basis Function under KD Tree Index Strategy[J]. Journal of System Simulation, 2016, 28(9): 2154-2158.
21. Cheng, X., Jia, D., Cheng, X. (2014). Theories and Technologies for Processing Massive Point Cloud Data. Shanghai: Tongji University Press.

 doi:10.20944/preprints202605.0620.v1

22. Li, B., Wei, J., Ma, B., et al. (2019). Volume Calculation of Irregular Bodies Using 3D Laser Point Cloud Slicing Method. Journal of Geodesy, 48(01), 42-52.
23. Wang, Y., Zhang, H., Wang, N. et al. Rotational-guided optimal cutting-plane extraction from point cloud. Multimed Tools Appl 79, 7135–7157 (2020). https://doi.org/10.1007/s11042-019-08339-w.
24. Ghazali R , Sukri A E , Latif A R A ,et al.Evaluating the relationship between scanning res-olution of laser scanner with the Becerik-Gerber B , Jazizadeh F , Kavulya G ,et al.Assessment of target types and layouts in 3D laser scanning for registration accuracy[J].Automation in Construction, 2011, 20(5):649-658.DOI:10.1016/j.autcon.2010.12.008.